TCOX8: TCS Metal Oxide Solutions Database

Database name:	TCS Metal Oxide Solutions Database	*Database acronym:*	TCOX
Database owner:	Thermo-Calc Software AB	*Database version:*	8.0

TCOX8 is a thermodynamic database for slags and oxides for use with Thermo-Calc and the add-on Diffusion Module (DICTRA) and/or Precipitation Module (TC-PRISMA). Developed using the CALPHAD approach, TCOX is based on the critical evaluation of binary, ternary and important higher order systems which enables predictions to be made for multicomponent systems. The database is the result of a long-term collaboration with academia. The first release of the database was in August 1992.

Included Elements (24)

Al	Ar	C	Ca	Co	Cr	Cu	F	Fe	Gd	La	Mg
Mn	Mo	Nb	Ni	O	P	S	Si	V	W	Y	Zr

Ar is only included in the gas phase.

The intended application is for solid and liquid ionized materials, e.g. oxides or sulfides. This could be development of ceramics, slags, refractories, metallurgical processing (e.g. slag and liquid metal interactions), ESR slags, materials corrosion, Thermal Barrier Coatings (TBC), Yttria-Stabilised-Zirconia (YSZ), solid oxide fuel cell materials, sulfide formation, dephosphorization and desulfurization, but the database is of course not limited to this. Despite the name of the database, it can be used even for fluoride and sulfide systems without oxygen. The liquid phase is described from liquid metal to oxide and/or fluoride, i.e. no pure liquid oxygen or fluorine is modeled. For sulfur, the liquid phase is described all the way from metal to sulfur.

TCOX has been developed in a CALPHAD spirit in order to give an accurate thermodynamic description of the multi-component systems of interest. In total, 241 binary systems and 218 ternary systems in this 24-element framework have been assessed to their full range of composition and temperature. In addition, TCOX also contains assessments of 88 pseudo-ternary oxide systems, 28 oxy-fluoride and oxy-sulfide systems, and some higher order systems as well. The systems and composition ranges which have been assessed are described below. The most accurate calculations will be obtained in or near these sub-systems and composition ranges.

However, intermetallic compounds and carbides are not included in the database. For solid phases, the TCOX database is compatible with TCFE Steels/Fe-Alloys Database, TCNI Ni-based Superalloys Database and SSOL Solutions Database. Thus, if needed, more metallic phases can be obtained by appending from TCFE, TCNI, SSOL and/or other appropriate databases. However, one must keep in mind that the LIQUID phase

from other databases and the IONIC_LIQ phase from TCOX should never be simultaneously considered in the same defined system/calculation, as they both represent the liquid phase using two different models. The binary O- and S-systems can be calculated with the BINARY module in Thermo-Calc.

TCOX contains 352 phases in total. The liquid metal and slag (IONIC_LIQ) is described with the ionic two-sublattice liquid model [1985, Hillert; 1991, Sundman] using a single Gibbs energy curve. The advantage with the ionic two-sublattice model is that it allows a continuous description of a liquid which changes in character with composition. The model has successfully been used to describe liquid oxides, silicates, sulfides, fluorides as well as liquid short range order, molten salts and ordinary metallic liquids. At low level of oxygen, the model becomes equivalent to a substitutional solution model between metallic atoms.

Different composition sets of IONIC_LIQ designated by #1, #2 etc. (e.g. IONIC_LIQ#1) may be observed which often represent the metallic and ionized liquid phases. Different composition sets also describe miscibility gaps frequently found in e.g. silicate systems. The #n suffix (where n is an integer) is generated dynamically by Thermo-Calc when using global minimization and therefore the identification of the phases should be determined from their compositions.

TCOX also contains solid oxides, silicates, fluorides and sulfides, a gaseous mixture phase and solid solution alloy phases (FCC_A1, BCC_A2 etc). Many phases are modeled as solution phases (in all cases where it is meaningful). The solid solution phases such as spinel, mullite, corundum, halite, olivine, fluorite etc. are modeled within the framework of the Compound Energy Formalism (CEF) [2001, Hillert]. The complete list of phases is given in Phases Included in TCOX.

Limits

As in the spirit of the CALPHAD method, predictions can be made for multicomponent systems by extrapolation into multicomponent space of data critically evaluated and assessed based on binary, ternary and in some cases higher order systems. However, critical calculations must always be verified by experimental data; it is the user's responsibility to verify the calculations but Thermo-Calc Software AB is interested to know about any significant deviations in order to improve any future release.

Database Revision History

If you are interested in the revision history for this database, the information is available in the online help (from Thermo-Calc go to **Help>Online Help**) or in the release notes on our website.

Assessed Systems

These are the assessed systems in the full range of composition and temperature.

Assessed Metallic Systems

All metal-metal binaries except Ca-W, Ca-Zr, Gd-La, Gd-P, La-Nb, La-P, La-Si, Mg-P, P-V, P-W and P-Zr are assessed. Many ternary metallic systems are also assessed. No intermetallic phases are included in the database. If needed, more solid phases can be appended from TCFE, TCNI, TCAL or other appropriate databases.

Assessed Binary Oxide Systems

Al-O	Ca-O	Co-O	Cr-O	Cu-O	Fe-O	Gd-O	La-O	Mg-O	Mn-O
Mo-O	Nb-O	Ni-O	P-O	Si-O	V-O	W-O	Y-O	Zr-O	

Assessed Ternary Oxide Systems, Me1-Me2-O

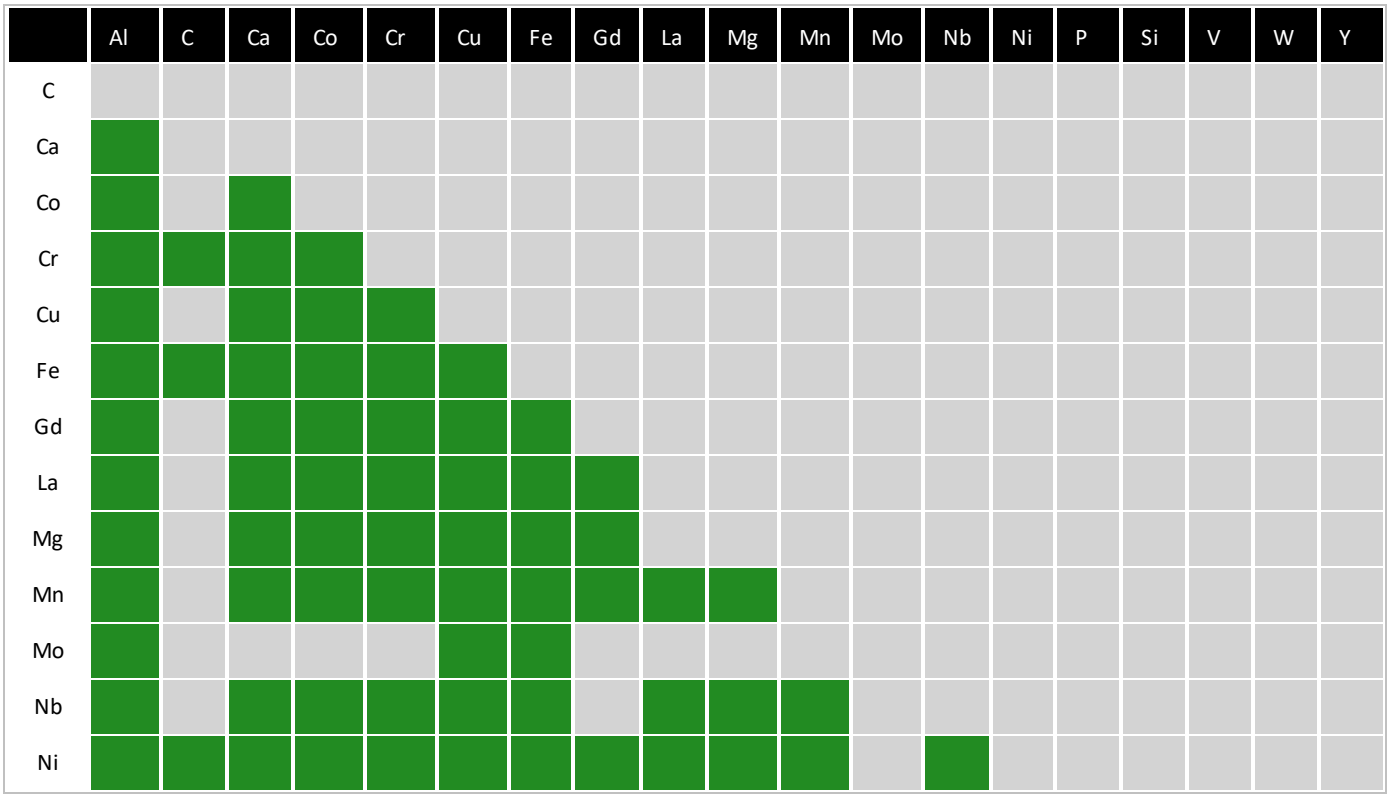

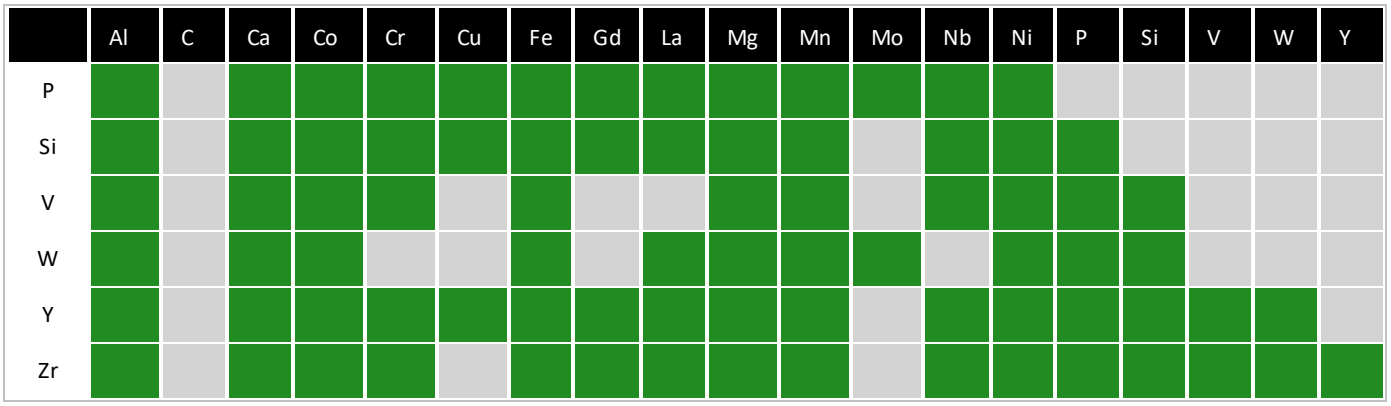

Assessed Quaternary Oxide Systems, Me1-Me2-Me3-O

Al-Ca-Co-O	Al-Ca-Cr-O	Al-Ca-Fe-O	Al-Ca-Mg-O	Al-Ca-Mn-O
Al-Ca-Nb-O	Al-Ca-Ni-O	Al-Ca-Si-O	Al-Ca-O-Si	Al-Ca-O-Y
Al-Ca-O-Zr	Al-Co-O-Si	Al-Cr-Fe-O	Al-Cr-Mg-O	Al-Cr-Ni-O
Al-Cr-O-Y	Al-Cu-O-Si	Al-Fe-Mg-O	Al-Fe-Mn-O	Al-Fe-O-Si
Al-Fe-O-Y	Al-Gd-O-Zr	Al-La-O-Y	Al-La-O-Zr	Al-Mg-O-P
Al-Mg-O-Si	Al-Mg-O-Y	Al-Mg-O-Zr	Al-Mn-O-Si	Al-O-P-Si
Al-O-Si-Y	Al-O-Si-Zr	Al-O-Y-Zr	Ca-Co-O-Si	Ca-Cr-Fe-O
Ca-Cr-O-Si	Ca-Cu-Fe-O	Ca-Cu-O-Si	Ca-Fe-Mg-O	Ca-Fe-Mn-O
Ca-Fe-O-P	Ca-Fe-O-Si	Ca-Gd-O-Si	Ca-Mg-Mn-O	Ca-Mg-O-P
Ca-Mg-O-Si	Ca-Mg-O-Zr	Ca-Mn-O-P	Ca-Mn-O-Si	Ca-Mn-O-Y
Ca-Nb-O-Si	Ca-Ni-O-Si	Ca-O-P-Si	Ca-O-Si-Y	Ca-O-Si-Zr
Ca-O-Y-Zr	Co-Cr-O-Si	Co-Cu-La-O	Co-Fe-La-O	Co-Fe-Mn-O
Co-Fe-O-P	Co-Fe-O-Si	Co-La-Ni-O	Co-Mg-O-Si	Co-Mn-O-Si
Co-Ni-O-Si	Cr-Fe-Mn-O	Cr-Fe-Ni-O	Cr-Fe-O-Y	Cr-La-Mn-O
Cr-Mg-O-Si	Cr-Mn-Ni-O	Cu-Fe-O-Si	Cu-Mg-O-Si	Fe-Mg-O-Si
Fe-Mn-O-Si	Fe-Ni-O-Si-O	Gd-La-O-Si	Gd-O-Si-Y-O	Gd-O-Si-Zr-O

La-O-Y-Zr	Mg-Mn-O-Si	Mg-Ni-O-Si	Mg-O-P-Si	Mg-O-Si-Y
Mg-O-Si-Zr	Mg-O-Y-Zr	Mn-O-Y-Zr		

Assessed Higher Order Oxide Systems

Al-Ca-Co-O-Si	Al-Ca-Fe-O-Si	Al-Ca-Mg-O-Si	Al-Ca-Mg-O-Zr
Al-Ca-O-Si-Y	Al-Fe-Mg-O-Si	Al-Fe-Mn-O-Si	Al-Gd-O-Y-Zr
Al-La-O-Y-Zr	Ca-Fe-Mg-O-Si	Ca-Mg-Ni-O-Si	Ca-Mg-O-P-Si
Gd-La-O-Y-Zr	C-Cr-Fe-Mn-Ni-O		

Assessed Binary Sulfide Systems

Al-S	Ca-S	Co-S	Cr-S	Cu-S	Fe-S	Gd-S	La-S	Mg-S
Mn-S	Mo-S	Nb-S	Ni-S	Si-S	V-S	W-S	Y-S	Zr-S

Assessed Ternary Sulfide Systems, Me1-Me2-S

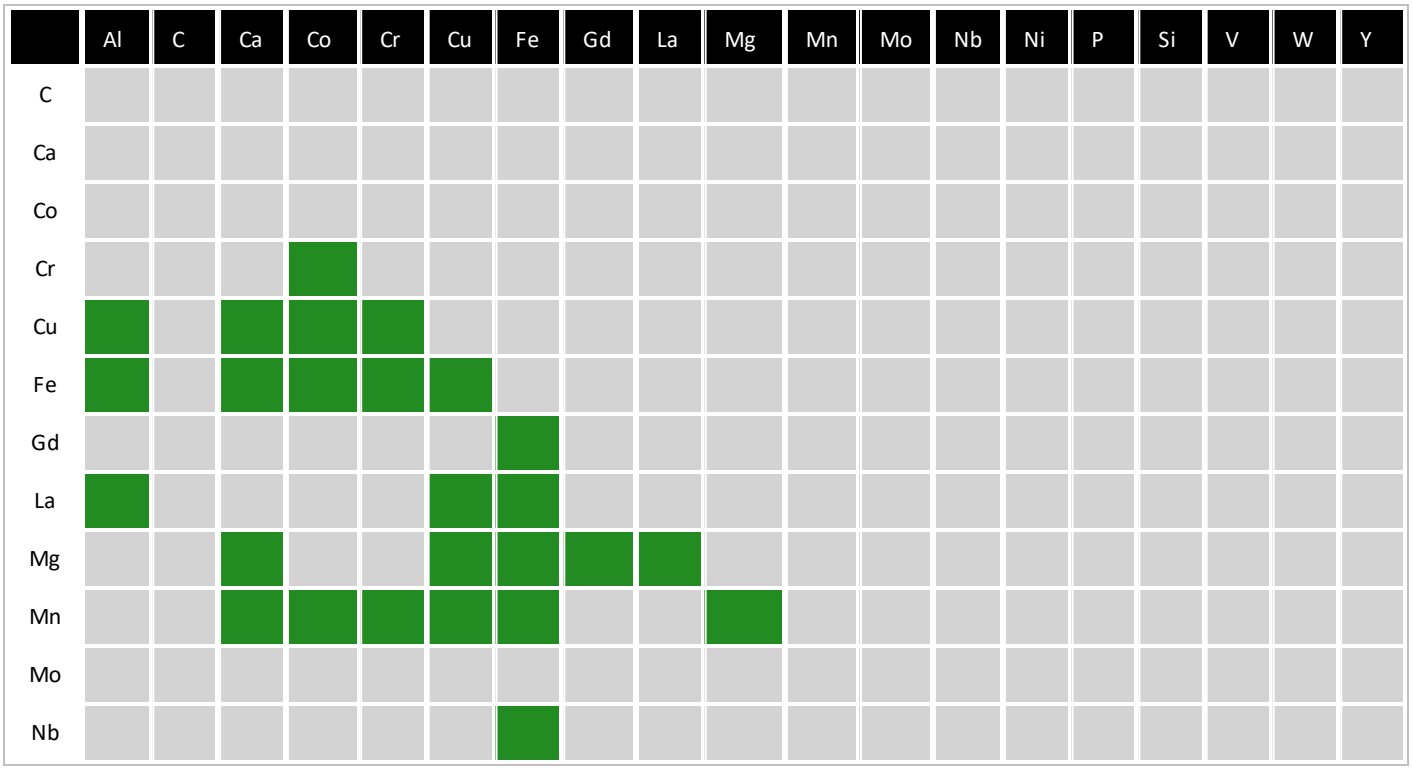

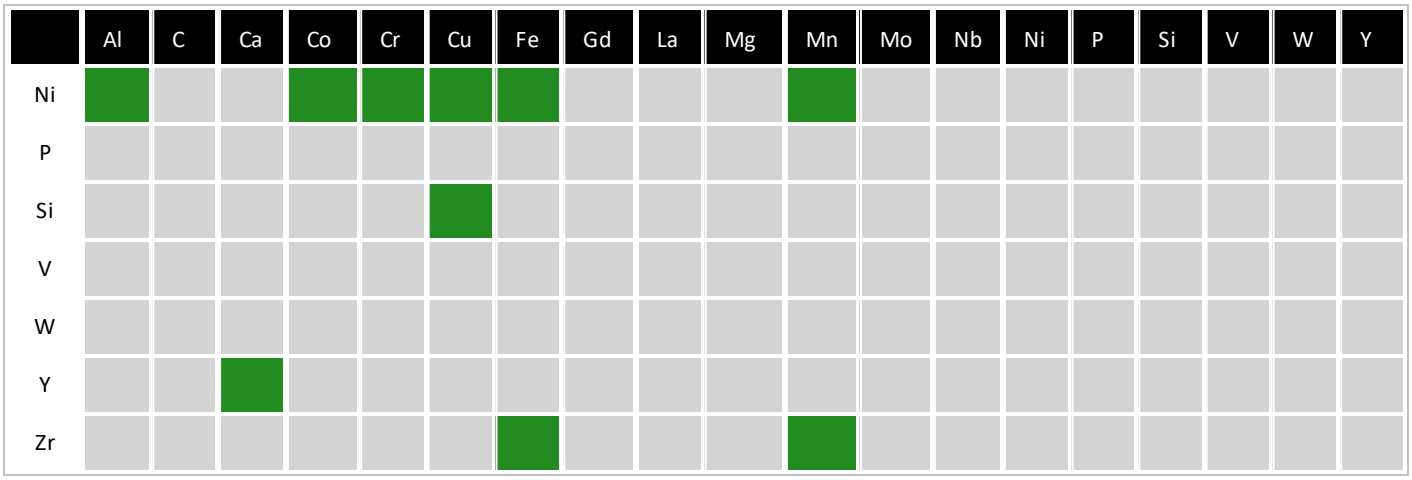

Assessed Oxy-sulfide Systems

Al-O-S	Ca-O-S	Co-O-S	Cr-O-S	Cu-O-S	Fe-O-S
Mg-O-S	Mn-O-S	O-S-Si	Al-Ca-O-S	Al-Mg-O-S	Al-Mn-O-S
Ca-Fe-O-S	Ca-Mg-O-S	Ca-O-S-Si	Cu-Fe-O-S	Fe-O-S-Si	Mg-O-S-Si
Mn-O-S-Si	Al-Ca-Mn-O-S				

Assessed Binary Fluoride Systems

AlF_3	Ca-F	CoF_2	CoF_3	CrF_2	CrF_3	CuF	CuF_2
FeF_2	FeF_3	GdF_3	LaF_3	MgF_2	MnF_2	MoF_4	
NbF_2	NbF_5	NiF_2	SiF_4	VF_2	YF_3	ZrF_4	

Assessed Ternary Fluoride Systems

Al-Ca-F	Al-F-Mg	Al-F-Zr	Ca-Co-F	Ca-Cr-F	Ca-Fe-F	Ca-F-Gd
Ca-F-La	Ca-F-Mg	Ca-F-Mn	Co-F-Gd	Co-F-Mg	Co-F-Ni	Fe-F-Ni
F-Gd-Mg	F-Gd-Y	F-La-Zr	F-Mg-La	F-Mg-Y		

Assessed Oxy-fluoride Systems

Al-F-O	Ca-F-O	Co-F-O	F-Mg-O	Al-Ca-F-O	Ca-F-Mg-F-O
Ca-Fe-F-O	Ca-F-O-P	Ca-F-O-Si	F-Mg-O-Si	Al-Ca-F-Mg-O	Al-Ca-F-O-Si

TCOX Calculation Examples

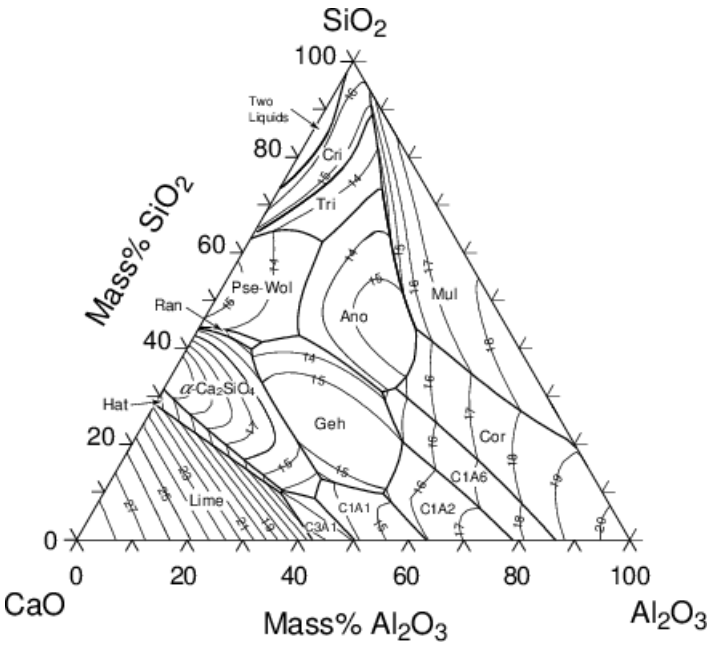

Figure 1: Calculated phase diagram of the CaO-Al_2O_3-SiO_2 system [2006, Mao]. Ano: anorthite, C1A1: $CaAl_2O_4$, C1A2: $CaAl_4O_7$, C1A6: $CaAl_{12}O_{19}$, C3A1: $Ca_3Al_2O_8$, Cor: corundum, Cri: cristobalite, Geh: gehlenite, Hat: hatrurite, Mul: mullite, Pse-Wol: pseudo-wollastonite, Ran: rankinite, Tri: tridymite.

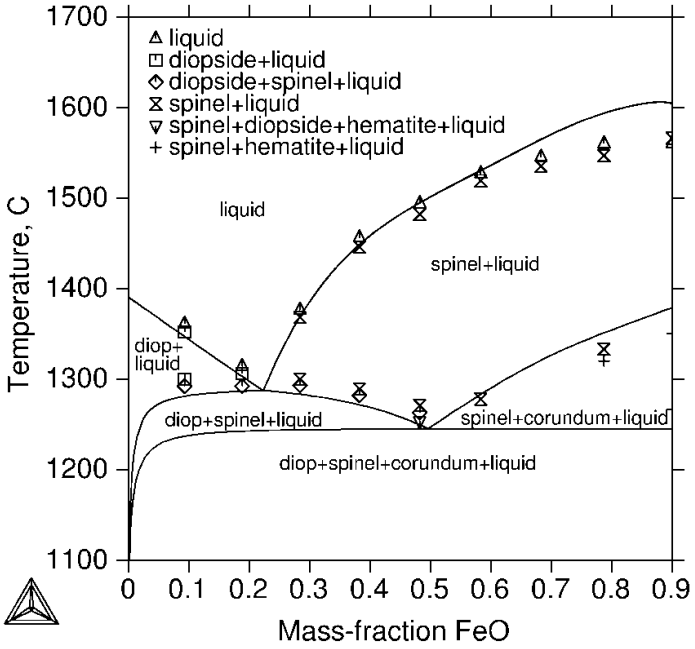

Figure 2: Calculated $CaMgSi_2O_6$ (diopside)-FeO_x section in air.

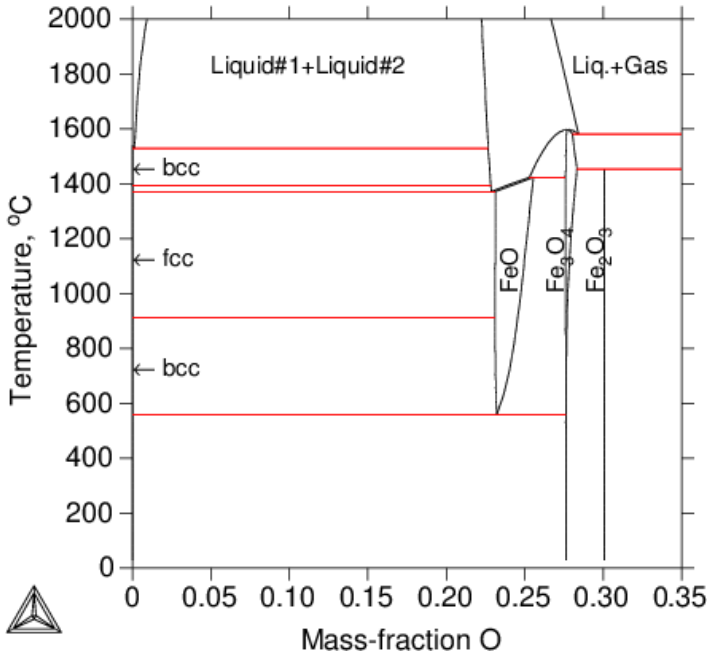

Figure 3: Calculated Fe-O phase diagram [1991, Sundman].

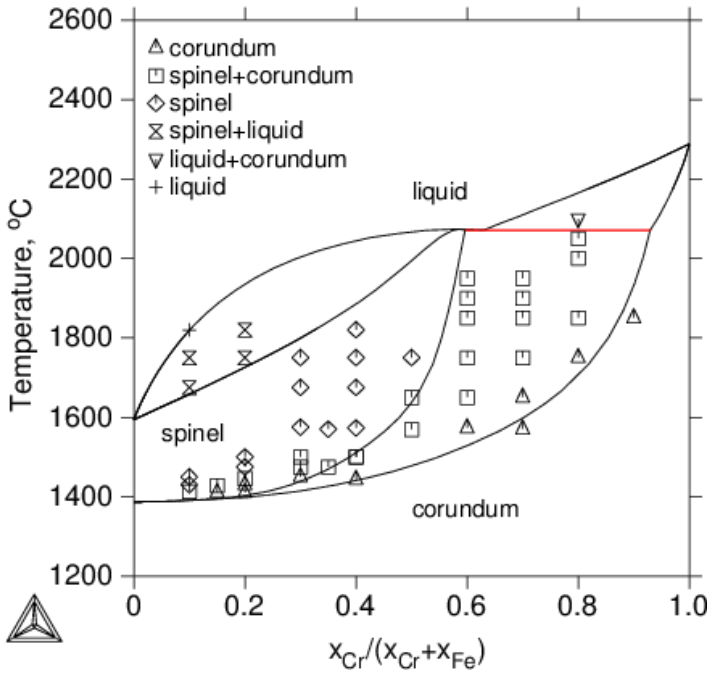

Figure 4: Calculated [2008, Kjellqvist] and experimental phase diagram of Cr-Fe-O in air [1960, Muan].

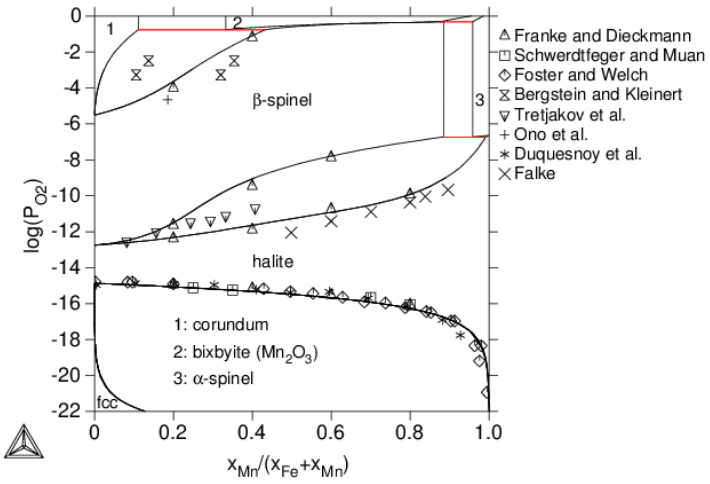

Figure 5: Calculated [2010, Kjellqvist] and experimental phase diagram of Fe-Mn-O at 1000 °C [1967, Schwerdt; 1990, Franke; 1956, Foster; 1971, Ono; 1975, Duquesnoy; 1987, Falke; 1964, Bergstein; 1965, Tretjakov].

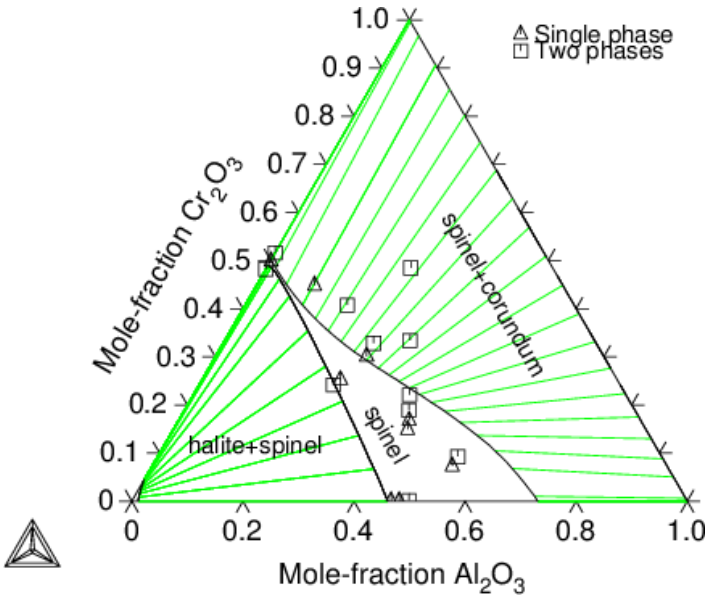

Figure 6: Calculated and experimental [1966, Greskovich] isothermal section of Al_2O_3-Cr_2O_3-MgO at 1700 °C and P_{O2}=1.

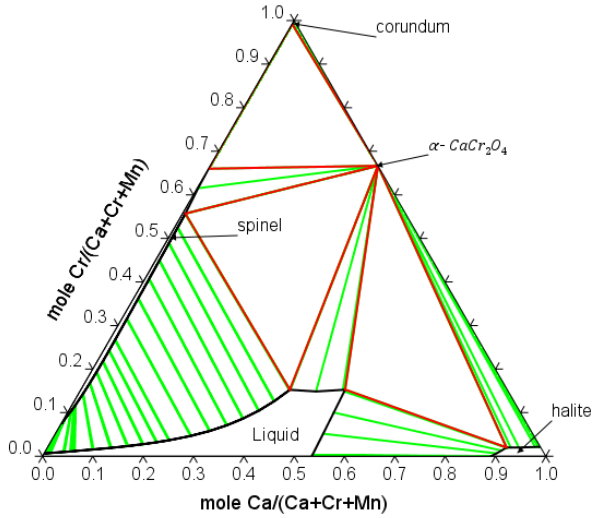

Figure 7: Isothermal section of CaO-Cr_2O_3-Mn_2O_3 calculated at 1600 °C in air.

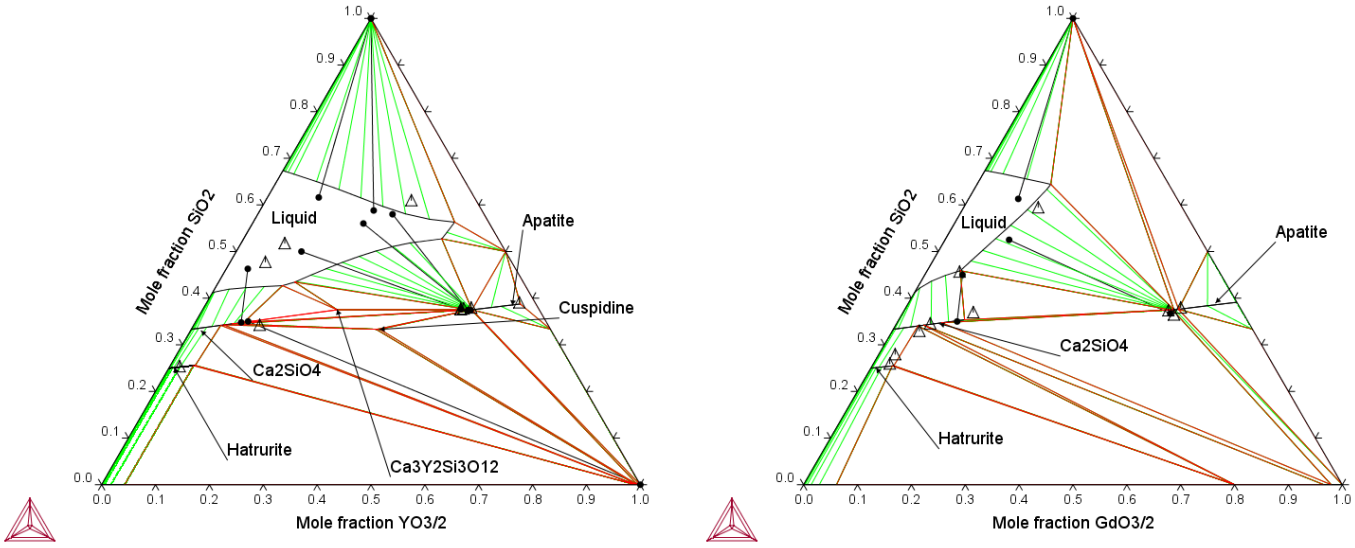

Figure 8: Calculated isothermal sections of CaO-SiO_2-$YO_{1.5}$ (left) and CaO-SiO_2-$GdO_{1.5}$ (right) at 1600 °C, compared to data on 3-phase corners and tie-lines from Poerschke [2017, 2016a, 2016b].

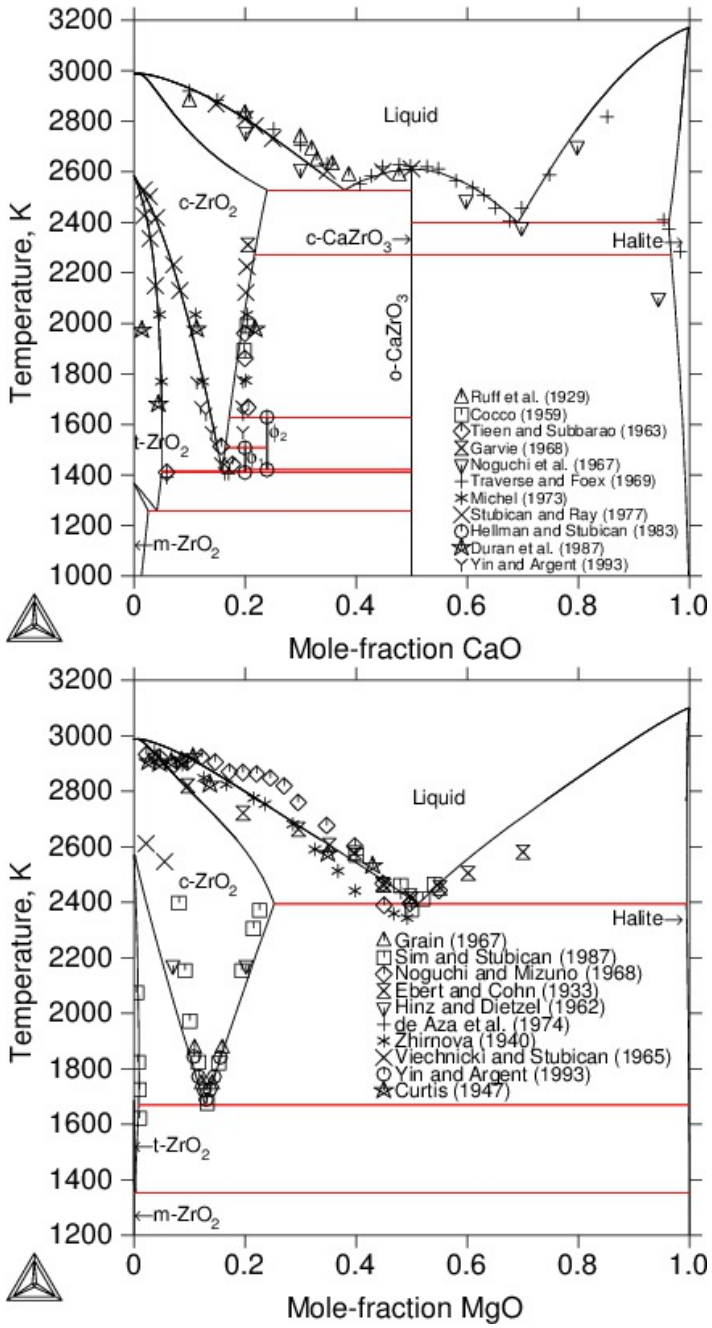

Figure 9: Calculated and experimental phase diagrams for CaO-ZrO_2 (top) and MgO-ZrO_2 (bottom) [see Figure 9 References].

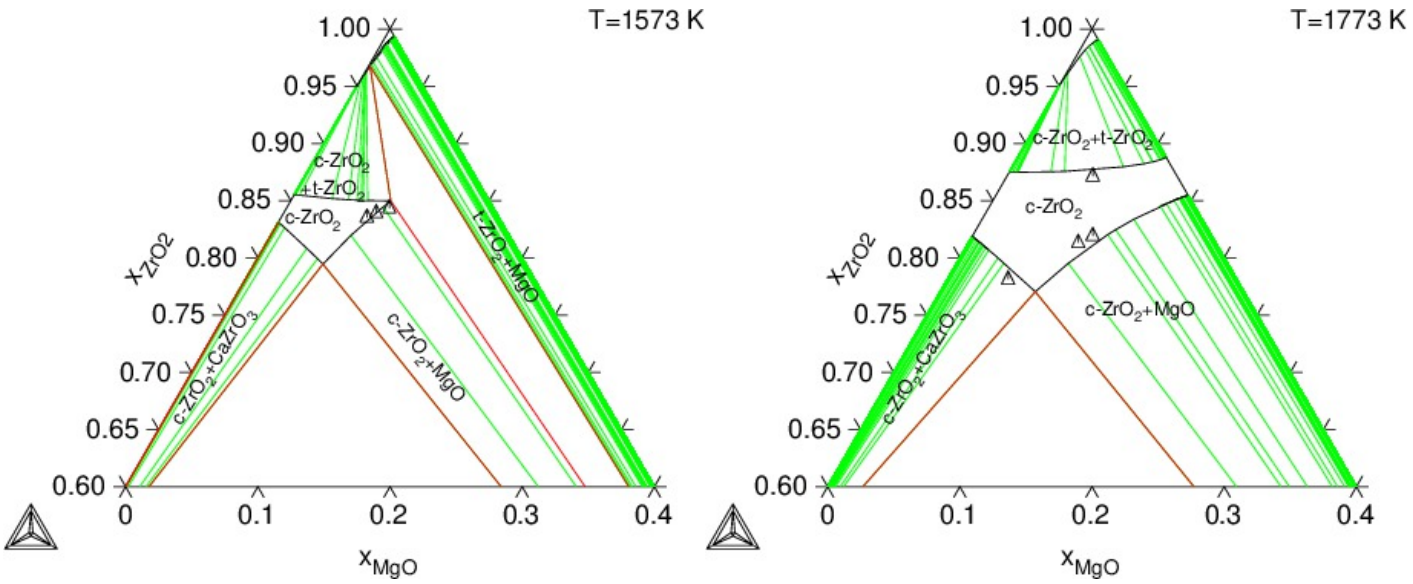

Figure 10: Isothermal sections of CaO-MgO-ZrO_2 calculated at 1300 °C and 1500 °C with experimental data [1993, Yin].

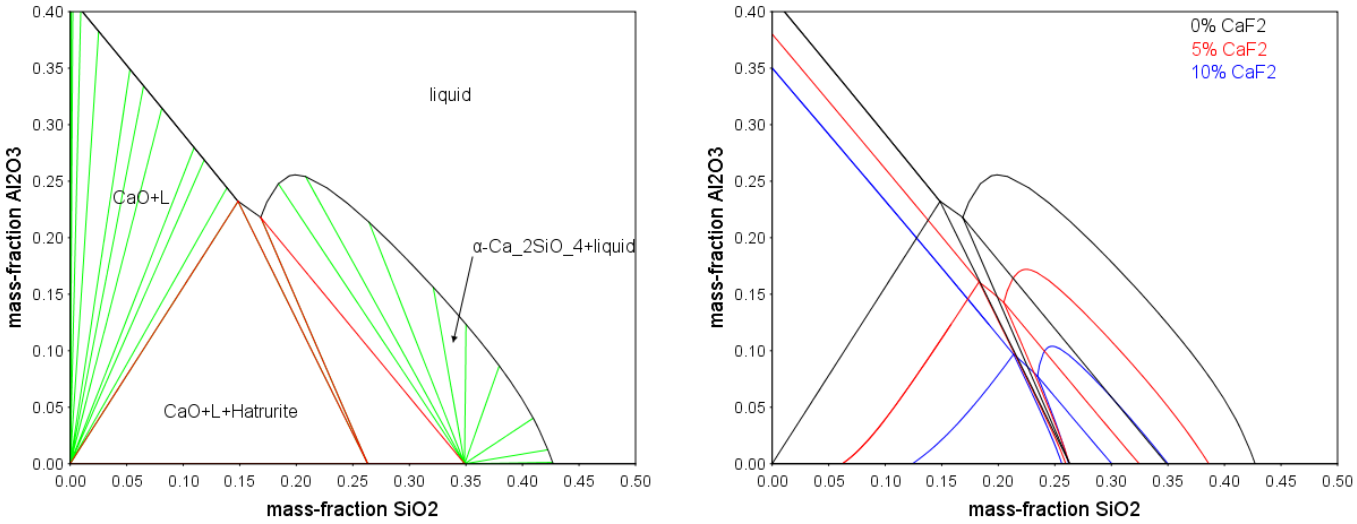

Figure 11: Calculated effect of CaF_2 on the Al_2O_3-CaO-SiO_2 system at 1600 °C.

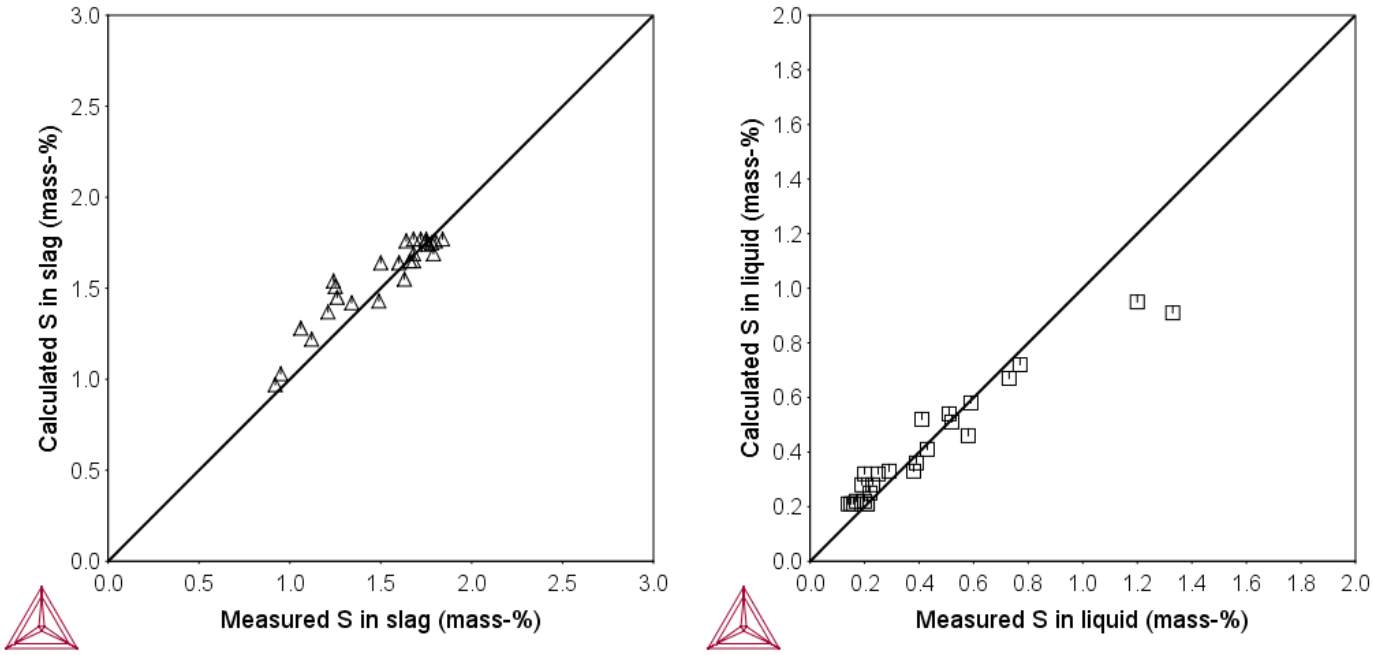

Figure 12: Sulfur in ladle slag. An impressive amount of sulfide capacity measurements have been made for a variety of slag systems over the years, but the results are very scattered. Allertz [2016] used a different method with equilibrium between copper and slag. Sulfur was added as Cu_2S. Different CMAS slags were then equilibrated with Cu and Cu_2S under controlled oxygen partial pressures. The equilibrium sulfur contents in the copper and slag were then analyzed.

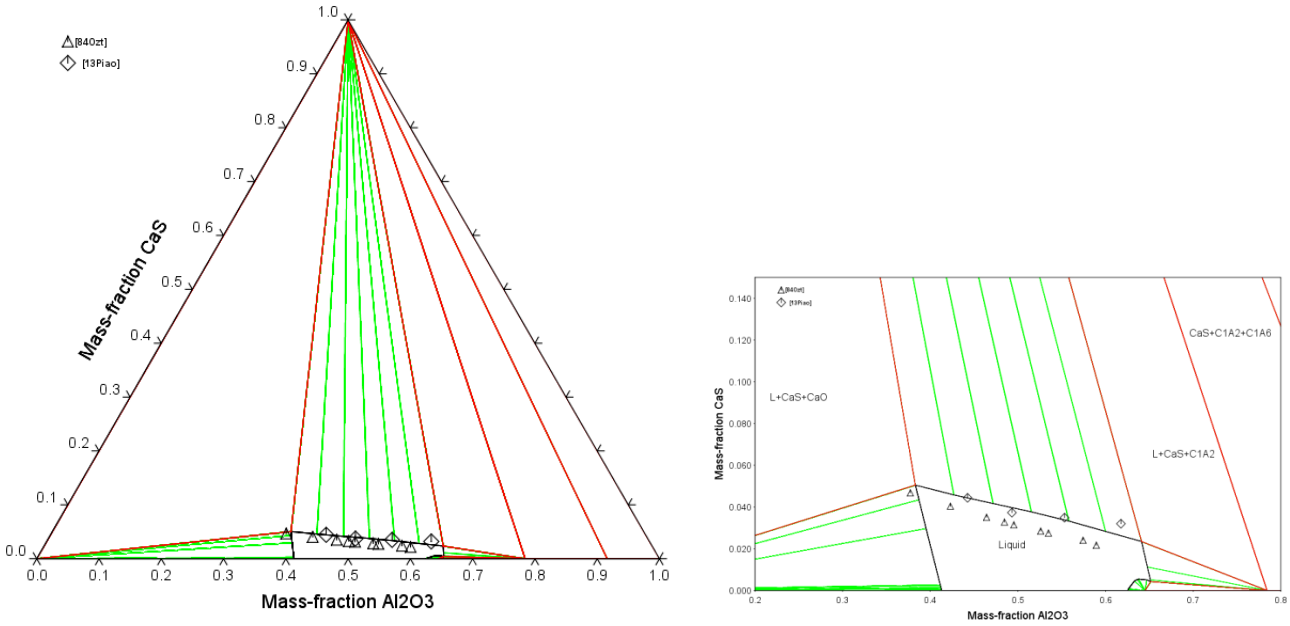

Figure 13: Isothermal section of the Al_2O_3-CaO-CaS system at 1600 °C with experimental data [1984, Ozturk; 2013, Piao].

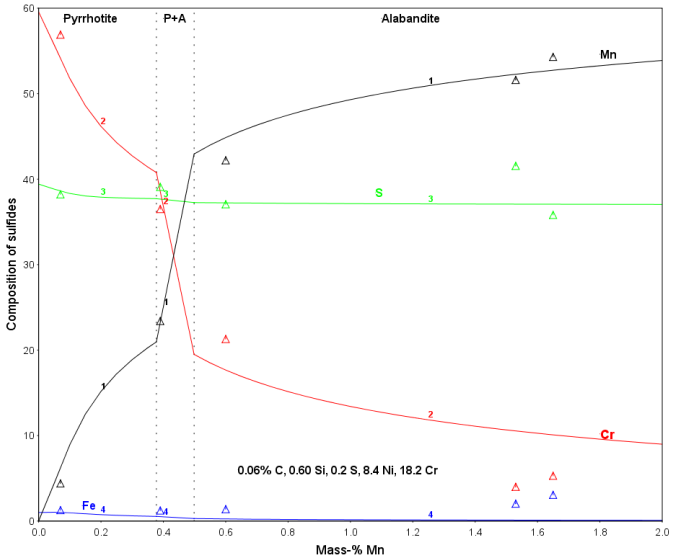

Figure 14: Calculated effect of inclusion composition of 18-8 stainless steel. The stability and composition of sulfides have been investigated [1980, Ono] at 1100 °C by varying the Mn concentraion of the steel: Fe - 0.06% C - 0.6% Si - 0.2% S - 8.4% Ni - 18.2% Cr.

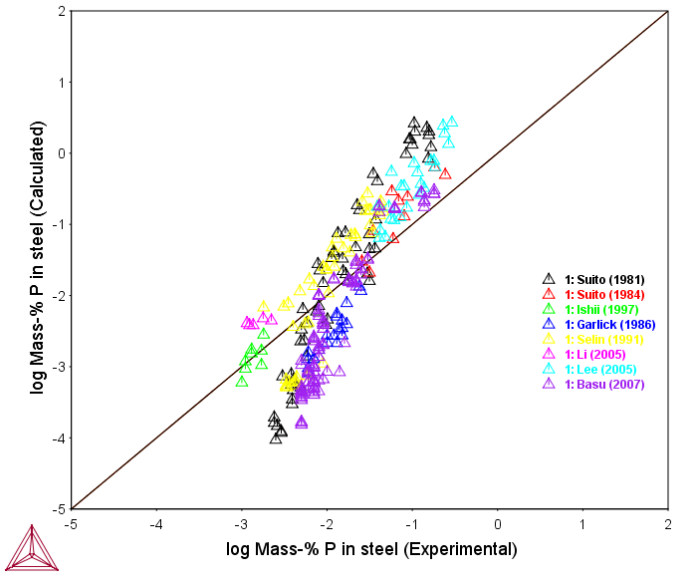

Figure 15: Comparison of experimental and calculated phosphorus solubility in liquid iron in equilibrium with slag in the Ca-Fe-Mg-O-P-Si system [see Figure 15 References].

Acknowledgement

Professor Malin Selleby, Dr. Bengt Hallstedt and David Dilner are acknowledged for many valuable discussions and important contributions.

TCOX References

[1956, Foster] P.K. Foster and A. J. E. Welch, “Metal-oxide solid solutions. Part 2. Activity relationships in solid solutions of ferrous oxide and manganous oxide,” Trans. Faraday Soc., vol. 52, 1636-1642, 1956.

[1960, Muan] A. Muan and S. Somiya, ”Phase Relations in the System Iron Oxide-Cr2O3 in Air. J. Am. Ceramic Soc., vol. 43(4), 204–209, 1960.

[1964, Bergstein] A. Bergstein and P. Kleinert, “Partial phase diagram of the system MnxFe3-xOy,” Collect. Czechoslov. Chem. Commun., vol. 29(10), 2549–2551, 1964.

[1965, Tretjakov] J.D. Tretjakov, Y.G. Saksonov, and I.V. Gordeev, "Chromite, Ferrite, Almninate,” Izv. Akad. Nauk. SSSR, Neorg. Mater., vol. 1, pp. 413-418, 1965.

[1966, Greskovich] C. Greskovich and V.S. Stubican, “Divalent chromium in magnesium-chromium spinels,” J. Phys. Chem. Solids, vol. 27(9), 1379–1384, 1966.

[1967, Schwerdt] K. Schwerdt and A. Muan, “Equilibria in System Fe-Mn-O Involving (Fe, Mn) O and (Fe, Mn) 3O4 Solid Solutions,” Trans. Metall. Soc. AIME, vol. 239(8), 1114–1119, 1967.

[1971, Ono] K. Ono, T. Ueda, T. Ozaki, Y. Ueda, A. Yamaguchi, and J. Moriyama, “Thermodynamic Study of the Fe-Mn-O System,” (in Japanese). Nippon Kinzoku Gakkai-Si, 38(8), 757–763, 1971.

[1975, Duquesnoy] A. Duquesnoy, J. Couzin, and P. Gode, “Isothermal Representation of Ternary Phase Diagrams ABO. Study of the System Mn-Fe-O,“ CR Acad. Sci. Paris C, vol. 281, 107–109, 1975.

[1980, Ono] K. Ono and T. Kohno, “Effect of Inclusion Composition on Stability of Inclusions and Corrosion Resistance of 18-8 Stainless Steel,” (in Japanese), Denki-Seiko, vol. 51, 122-131, 1980.

[1984, Ozturk] B. Ozturk and E.T. Turkdogan, “Equilibrium S distribution between molten calcium aluminate and steel, “Metal. Sci., vol. 18(6), 299-305, 1984.

[1985, Hillert] M. Hillert, B. Jansson, B. Sundman, and J. Ågren, “A two-sublattice model for molten solutions with different tendency for ionization,” Metall. Trans. A, vol. 16(1), 261–266, 1985.

[1987, Falke] H. Falke, Universität Hannover, Doctoral Thesis, 1987.

[1990, Franke] P. Franke and R. Dieckmann, “Thermodynamics of iron manganese mixed oxides at high temperatures,” J. Phys. Chem. Solids, vol. 51(1), 49–57, 1990.

[1991a, Sundman] B. Sundman, “Modification of the two-sublattice model for liquids,”Calphad, vol. 15(2), 109–119, 1991.

[1991b, Sundman] B. Sundman, “An assessment of the Fe-O system,” J. Phase Equilibria, vol. 12(2), 127–140, 1991.

[1993, Yin] Y. Yin and B.B. Argent, “The phase diagrams and thermodynamics of the ZrO2-CaO-MgO and MgO-CaO systems,” J. Phase Equilibria, vol. 14(5), 588–600, 1993.

[2001, Hillert] M. Hillert “The compound energy formalism,” J. Alloys Compd., vol. 320(2), 161–176, 2001.

[2006, Mao] H. Mao, M. Hillert, M. Selleby, and B. Sundman, “Thermodynamic Assessment of the CaO-Al2O3-SiO2 System,” J. Am. Ceramic Soc., vol. 89(1), 298–308, 2006.

[2008, Kjellqvist] L. Kjellqvist, M. Selleby, and B. Sundman, “Thermodynamic modelling of the Cr–Fe–Ni–O system, “Calphad, vol. 32(3), 577–592, 2008.

[2010, Kjellqvist] L. Kjellqvist and M. Selleby, ”Thermodynamic Assessment of the Fe-Mn-O System,” J. Phase Equilibria Diffus., vol. 31(2), 113–134, 2010.

[2013, Piao] R. Piao, H. Lee, and Y. Kang, “Experimental investigation of phase equilibria and thermodynamic modeling of the CaO–Al2O3–CaS and the CaO–SiO2–CaS oxysulfide systems,” Acta Mater., vol. 61(2), 683-696, 2013.

[2016, Allertz] C. Allertz, “Sulfur and Nitrogen in Ladle Slag”, PhD. thesis, KTH Royal Institute of Technology, Stockholm, Sweden, 2016.

[2016a, Poerschke] D.L. Poerschke, T.L. Barth, O. Fabrichnaya, and C.G. Levi, “Phase equilibria and crystal chemistry in the Calcia-Silica-Yttria system,” J. Eur. Ceram. Soc., vol. 36(7), 1743-1754, 2016.

[2016b, Poerschke] D.L. Poerschke, T.L. Barth, and C.G. Levi, “Equilibrium relationships between thermal barrier oxides and silicate melts,” Acta Mater., vol. 120, 302-314, 2016.

[2017, Poerschke] D.L. Poerschke and C.G. Levi, “Phase equilibria in the Calcia-Gadolinia-Silica system,“ J. Alloys Compd., vol. 695, 1397-1404, 2017.

Figure 9 References

[1929, Ruff] O. Ruff, F. Ebert, and E. Stephan,”Beiträge zur Keramik hochfeuerfester Stoffe II. Das System ZrO2-CaO,” Zeitschrift fur Anorg. und Allg. Chemie, vol. 180(1), 215–224, 1929.

[1933, Ebert] F. Ebert and E. Cohn, “Beiträge zur Keramik hochfeuerfester Stoffe. VI. Das System ZrO2-MgO,” Zeitschrift fur Anorg. und Allg. Chemie, vol. 213(4), 321–332, 1933.

[1940, Zhirnova] N. Zhirnova, Zh. Prikl. Khim. 12, pp. 1278, 1940.

[1959, Cocco] A. Cocco, “Composition Limits at High Temperatures of the Cubic Phase Composed of ZrO 2 and CaO,” Chim. Ind.(Milan), vol. 41(9), 882–886, 1959.

[1962, Hinz] I. Hinz, A. Dietzel, and H. Meyer, “Die Phasengrenze der kubischen ZrO2-MgO-Mischkristalle von 1800 C bis zum Schmelzpunkt,” Ber. Dtsch. Keram. Ges, 39, 530–533, 1962.

[1962 Tien] T.Y. Tien and E.C. Subbarao, ”X-Ray and Electrical Conductivity Study of the Fluorite Phase in the System ZrO2[Single Bond]CaO,” J. Chem. Phys., vol. 39(4), 1041, 1963.

[1965, Viechnicki] D. Viechnicki and V.S. Stubican, “Mechanism of Decomposition of the Cubic Solid Solutions in the System ZrO2-MgO,” J. Am. Ceram. Soc., vol. 48(6), 292–297, 1965.

[1967, Grain] C.F. Grain, “Phase Relations in the ZrO2-MgO System,” J. Am. Ceram. Soc., vol. 50(6), 288–290, 1967.

[1967, Noguchi] T. Noguchi, M. Mizuno, and W.M. Conn, “Fundamental research in refractory system with a solar furnace—ZrO2-CaO system,” Solar Energy, vol. 11(3-4), 145–152, 1967.

[1968, Garvie] R.C. Garvie, “The Cubic Field in the System CaO-ZrO 2,” J. Am. Ceram. Soc., vol. 51(10), 553–556, 1968.

[1968, Noguchi] T. Noguchi and M. Mizuno, “Liquidus Curve Measurements in the ZrO2-MgO System with the Solar Furnace,” Bull. Chem. Soc. Jpn., vol. 41(7), 1583–1587, 1968.

[1969, Traverse] J.P. Traverse and M. Foex, “The Zirconia–Strontia and Zirconia–Lime Systems,” High Temp. High Press., vol. 1(4), 409–427, 1969.

[1973, Michel] D. Michel, “Etats d’ordre dans la solution solide de type fluorite du systeme zircone - chaux pour la composition 4 ZrO2 – CaO,” Mater. Res. Bull., vol. 8(8), 943–949, 1973.

[1974, de Aza] S.D. de Aza, C. Richmond and J. White, “Compatibility Relationships of Periclase in System CaO-MgO-ZrO2-SiO2,” Trans. J. Br. Ceram. Soc., vol. 73(4), 109–116, 1974.

[1977, Stubican] V. S. Stubican and S.P. Ray, “Phase Equilibria and Ordering in the System ZrO2-CaO,” J. Am. Ceram. Soc., vol. 60(11-12), 534–537, 1977.

[1983, Hellmann] J.R. Hellmann and V.S. Stubican, “Phase Relations and Ordering in the Systems Mg0-Y203-Zr02 and Ca0-Mg0-ZrO,” J. Am. Ceram. Soc., vol. 66(4), 260–264, 1983.

[1987, Duran] P. Duran, P. Recio, and J.M. Rodriguez, “Low temperature phase equilibria and ordering in the ZrO2-rich region of the system ZrO2-CaO,” J. Mater. Sci., vol. 22(12), 4348–4356, 1987.

[1987, Sim] S. M. Sim and V. S. Stubican, “Phase Relations and Ordering in the System ZrO2-MgO,” J. Am. Ceram. Soc., 70(7), 521–526, 1987.

[1993, Yin] Y. Yin and B.B. Argent “Phase diagrams and thermodynamics of the systems ZrO2-CaO and ZrO2-MgO,” J. Phase Equilibria, vol. 14(4), 439–450, 1993.

Figure 15 References

[1981, Suito] H. Suito, R. Inoue and M. Takada, "Phosphorus distribution between liquid iron and Mgo saturated slags of the system CaO-MgO-FeOx-SiO2", Trans. Iron Steel Inst. Japan, vol. 21, 250-259, 1981.

[1984, Suito] H. Suito and R. Inoue, "Phosphorus distribution between Mgo saturated CaO-FeOx-SiO2-P2O5-MnO slags and liquid iron", Trans. Iron Steel Inst. Japan, vol. 24, 40-46, 1984.

[1986, Garlick] C. Garlic, S. Jahanshahi and G.R. Belton, unpublished work, BHP Central Research Laboratories, Shortland, Australia, 1986 (cited in Chen et al., 2013)

[1991, Selin] R. Selin, "Studies on MgO solubility in complex steelmaking slags in equilibrium with liquid iron and distribution of phosphorus and vanadium between slag and metal at MgO saturation", Scand. J. Metall., vol 20, 279-299, 1991.

[1997, Ishii] H. Ishii and R.J. Fruehan, "Dephosphorization equilibria between liquid iron and highly basic CaO-based slags saturated with MgO", Iron Steelmaking, vol 24, 47-54, 1997.

[2005, Li] G. Li, T. Hamano and F. Tsukihashi, "The effect of Na2O and Al2O3 on dephosphorization of molten steel by high basicity MgO saturated CaO-FeOx-SiO2 slag", ISIJ Int., vol 45, 12-18, 2005.

[2005, Lee] C.M. Lee and R.J. Fruehan, "Phosphorus equilibrium between hot metal and slag", Ironmaking Steelmaking Process. Prod. Appl., vol 32, 503-508, 2005.

[2007, Basu] S. Basu, A.K. Lahiri and S. Seetharaman, "Phosphorus partition between liquid steel and CaO-SiO2-P2O5-MgO slag containing low FeO", Metall. Mater. Trans. B, vol 38, 357-366, 2007.

[2013, Chen] Chen, L. Zhang and J. Lehmann, "Thermodynamic modelling of phosphorus in steelmaking slags", High Temp. Mater. Process., vol 32, 237-246, 2013.

Phases Included in TCOX

In total there are 352 phases in the databases. Phases and constituents can be listed in the DATABASE module and the GES module. To show models and constituents for the phases in a chosen system, use the command LIST-SYSTEM with the option CONSTITUENTS in the Database module.

The Liquid Solution

The liquid phase contains all elements in the TCOX database. The ionic two-sublattice liquid model is used. The model may thus be used to describe liquid metal, oxides, sulfides, sulfur, fluoride, silicates etc. with the following formula:

$(Al^{+3}, Ca^{+2}, Co^{+2}, Cr^{+2}, Cu^{+1}, Fe^{+2}, Gd^{+3}, La^{+3}, Mg^{+2}, Mn^{+2}, Mo^{+4}, Nb^{+2}, Ni^{+2}, P^{+5}, Si^{+4}, V^{+2}, W^{+6}, Y^{+3}, Zr^{+4})_P$ $(AlO_2^{-1}, F^{-1}, O^{-2}, PO_4^{-3}, S^{-2}, SiO_4^{-4}, SO_4^{-2}, Va, C, C_3S_2Z_{1/6}, CoF_3, CoO_{3/2}, CrF_3, CrO_{3/2}, CuF_2, CuO, FeF_3, FeO_{3/2}, M_3S_2Z_{1/6}, MnO_{3/2}, NbF_5, NbO_2, NbO_{5/2}, PO_{5/2}, S, SiO_2, VO_2, VO_{3/2}, VO_{5/2})_Q$

Alloy Phases

BCC_A2

Containing Al, Ca, Co, Cr, Cu, Fe, Gd, La, Mg, Mn, Mo, Nb, Ni, P, S, Si, V, W, Y and Zr with C and O modeled interstitially.

FCC_A1

Containing Al, Ca, Co, Cr, Cu, Fe, Gd, La, Mg, Mn, Mo, Nb, Ni, P, S, Si, V, W, Y and Zr with C and O modeled interstitially.

HCP_A3

Containing Al, Ca, Co, Cr, Cu, Fe, Gd, La, Mg, Mn, Mo, Nb, Ni, Si, V, W, Y and Zr with C and O modeled interstitially.

DHCP

La phase dissolving Al, Ca, Cu, Gd, Mg, Mn, Ni and Y with O modeled interstitially.

CUB_A13

β-Mn, containing Al, Co, Cr, Fe, Mg, Mo, Nb, Ni, Si, V and Zr with C modeled interstitially.

CBCC_A12

α-Mn, containing Al, Co, Cr, Fe, Mg, Mo, Nb, Ni, Si, V and Zr with C modeled interstitially.

DIAMOND_FCC_A4

Diamond structure based on Si containing Al, C and P with O modeled interstitially.

GRAPHITE

This is pure carbon.

RED_P, WHITE_P

This is pure phosphor. Phosphor exists in two modifications: white (not stable at normal conditions) and red (up to the melting temperature of 579 ºC).

ORTHORHOMBIC_S, MONOCLINIC_S

This is pure sulfur. Sulfur exists in two modifications: orthorhombic (up to 95 ºC) and monoclinic (up to the melting temperature of 115 ºC).

Gas Phase

A reduced gas phase containing AL1F3, AR, C1O1, C1O2, CA1F2, F, F2, O, O10P4, O1P1, O2P1, O1S1, O2, O2S1, O3S1, O5P2, P2, P4 and S2.

Solid Solutions

The solid solution phases are modeled within the framework of the Compound Energy Formalism (CEF) [3]. These models take into account distribution of cations between sublattices, defects such as vacancies, anti-sites and ordering. 135 solutions are modeled in the database.

Alabandite

This is CaS (oldhamite), MnS (alabandite), MgS, GdS, LaS and ZrS solid solution.

$AlPO_4$

There are three modifications (S1, S2 and S3)of $AlPO_4$ with solubility of SiO_2.

α-Spinel

This is low-temperature tetragonal Mn_3O_4 solid solution dissolving Al, Co, Cr, Cu, Fe, Mg and Ni. Distribution of cations between tetrahedral and octahedral sites, as well as vacancies on the octahedral sites to model deviation from the ideal stoichiometry toward higher oxygen potential and interstitial Mn to model deviation toward excess manganese are taken into account.

Anhydrite

This is $(Ca,Cu,Fe,Mg,Mn,Ni)SO_4$.

Apatite

This is $(Ca,Mg)_2(Gd,Y)_8(SiO_4)_6O_2$ solid solution dissolving Zr.

β-V-O

This is β-V-O.

Bronze

This is $(Ca,Fe)_xV_2O_5$ bronze.

Calcium ferro-aluminates

C3A1: This is $Ca_3Al_2O_6$ dissolving ferric Fe.

C12A7: This is $Ca_{12}Al_{14}O_{32}$ dissolving ferric Fe. C12A7 is not stable in the anhydrous $CaO\text{-}Al_2O_3$ system. It is, however, important in practice, and included in the database. In the optimization it was treated as if it does not contain any water.

C1A1: This is $CaAl_2O_4$ dissolving ferric Fe.

C1A2: This is $CaAl_4O_7$ dissolving ferric Fe.

C1A6: This is $CaAl_{12}O_{19}$ dissolving ferric Fe.

C1A1F2: This is $Al_2CaFe_4O_{10}$ with a variation in Al/Fe: $CaAlFe_2(Al,Fe)_3O_{10}$.

C2F: This is $Ca_2Fe_2O_5$ dissolving Al.

$Ca_3P_2O_8$ (α and β)

α-$Ca_3P_2O_8$ dissolving Mg and Si and β-$Ca_3P_2O_8$ dissolving Mg.

$Ca_2P_2O_7$ (α, β and γ)

α, β and γ-$Ca_2P_2O_7$ dissolving Mg.

Ca_2SiO_4 (α and α')

α-Ca_2SiO_4- α'-$Ca_3P_2O_8$ dissolving Gd, Mg, Mn, Y and α'-Ca_2SiO_4 dissolving Fe, Gd, Mg, Mn, P and Y.

$Ca_3S_3Fe_4O_x$

This is the oxy-sulfide $3CaS.4FeO\text{-}3CaS.4Fe_2O_3$.

$Ca_3Y_2Si_3O_{12}$

This is $Ca_3(Gd,Y)_2(SiO_4)_3$.

$Ca_3Y_2Si_6O_{18}$

This is $Ca_3(Gd,Y)_2(SiO_4)_6$.

$Ca_4Nb_2O_9$_HT11

This is the high-temperature $Ca_4Nb_2O_9$ phase with excess CaO.

$Ca_4Nb_2O_9$_LT21

This is the low-temperature $Ca_4Nb_2O_9$ phase with excess CaO.

$Ca_3Co_2O_6$

This is $Ca_3Co_2O_6$ dissolving Cu.

$Ca_3Co_4O_9$

This is $Ca_3Co_4O_9$ dissolving Cu.

$CaCr_2O_4$_A

This is the high-temperature $CaCr_2O_4$ dissolving Al and Fe.

CaF_2_S1

This is low-temperature CaF_2 dissolving CaO and MgF_2.

CaF_2_S2

This is high-temperature CaF_2 and CuF_2 dissolving CaO and MgF_2.

$Ca_3Mg_3P_4O_{16}$

This is $Ca_3Mg_3P_4O_{16}$.

$CaMO_3$

This is $CaMnO_3$ and low-temperature $CaZrO_3$ dissolving Y.

$Ca_5P_2SiO_{12}$

This is $Ca_5P_2SiO_{12}$.

CaSFeO

This is the oxy-sulfide CaS.FeO-CaS.Fe_2O_3.

$CaSO_4$_HT

This is (Ca,Co,Mg)SO_4.

CaV_2O_4

This is $CaFe_2O_4$, β-$CaCr_2O_4$, CaV_2O_4 and CaY_2O_4 solid solution dissolving Al. Prototype phase is CaV_2O_4.

CaV_2O_6

This is (Ca,Mg,Mn)V_2O_6.

CaY_4O_7

This is Ca(Gd,Y)$_4O_7$.

$CaYAl_3O_7$

This is Ca(Gd,Y)Al_3O_7.

$CaYAlO_4$

This is Ca(Gd,Y)AlO_4.

$CaZrO_3$_C

This is the cubic high-temperature $CaZrO_3$ phase dissolving Y.

Chalcopyrite

This is an intermediate solid solution phase in the Cu-Fe-S system around the composition $CuFeS_2$.

Co_9S_8

This is Co_9S_8 dissolving Fe and Ni.

Columbite

This is (Ca,Co,Fe,Mg,Mn)Nb_2O_6 with excess FeO and MgO.

Cordierite

This is Al_4(Fe,Mg,Mn)$_2Si_5O_8$.

Corundum

This is Corundum (Al_2O_3), Eskolaite (Cr_2O_3), Hematite (Fe_2O_3) and Karelianite (V_2O_3) solid solution dissolving Mn and Ni.

Cr_2S_3

This is Cr_2S_3 dissolving Fe.

Cr_3S_4

This is Cr_3S_4 dissolving Fe, Mn and Ni.

$CrNbO_4$

This is $CrNbO_4$ solid solution with excess Cr_2O_3 and Nb_2O_5.

$Cr_2P_4O_{13}$

This is $Cr_2P_4O_{13}$ and $(Cr,Fe)_2V_4O_{13}$.

CuF_2

This is CrF_2 and low temperature CuF_2.

$CuLa_2O_4$

This is $CuLa_2O_4$ with solubility of Co.

CuP_2O_6

This is $(Co,Cu,Ni)P_2O_6$.

CuO

This is CuO with solubility of Co.

Cristobalite

This is SiO_2 with solubility of $AlPO_4$.

Delafossite

This is $Cu(Al,Cr,Fe,La,Mn,Y)O_2$.

Digenite

This is Cu_2S solid solution with excess S and solubility of Fe, Mg and Mn.

$DyMn_2O_5$

This is $Mn_2(Gd,Y)O_5$ solid solution. Prototype phase is $DyMn_2O_5$.

FeF_3

This is $(Al,Co,Cr,Fe)F_3$.

$Fe_2O_{12}S_3$

This is the oxy-sulfides $(Al,Cr,Fe)_2(SO_4)_3$.

$FeNb_{14}O_{36}$

This is $(Co,Fe)Nb_{14}O_{36}$.

$FeNb_{36}O_{91}$

This is $(Co,Fe)Nb_{36}O_{91}$.

$FeNb_{68}O_{171}$

This is $(Co,Fe)Nb_{68}O_{171}$.

$FePO_4$

This is $(Fe,Mn)PO_4$.

$FeVO_4$

This is $(Al,Fe)VO_4$.

Fluorite

This is high-temperature ZrO_2 solid solution with solubility of Al, Ca, Cr, Fe, Gd, La, Mg, Mn, Ni, Si and Y.

Garnet

This is grossular ($Ca_3Al_2Si_3O_{12}$), uvarovite ($Ca_3Cr_2Si_3O_{12}$) and spessartine ($Mn_3Al_2Si_3O_{12}$).

GdF_3

This is high temperature $(Gd,Y)F_3$.

$Gd_2Si_2O_7$

This is $(Gd,La)_2Si_2O_7$.

Gd_2SiO_5

This is $(Gd,La)_2SiO_5$.

Halite

This is Lime (CaO), CoO, Wustite (FeO), Periclase (MgO), Manganosite (MnO), bunsenite (NiO) and VO solid solution dissolving also Al, Cu, Cr, Gd, Y and Zr.

Hatrurite

This is Ca_3SiO_5 dissolving Gd and Y.

β1-Heazlewoodite

This is non-stoichiometric high-temperature Ni_3S_2 dissolving Co and Fe.

β2-Heazlewoodite

This is non-stoichiometric high-temperature Ni_4S_3 dissolving Fe.

LaF_3

This is low temperature $(Gd,La,Y)F_3$.

La_2S_3

This is $(Gd,La)_2S_3$.

La_2MnO_4

This is $La_2(Mn,Ni)O_4$ solid solution dissolving Co.

$La_3Ni_2O_7$

This is $La_3Ni_2O_7$ dissolving Co.

$La_4Ni_3O_{10}$

This is $La_4Ni_3O_{10}$ dissolving Co.

LaAP

This is a rhombohedral perovskite, $La(Al,Co)O_3$ dissolving Ca, Cu, Ni and Y.

LaYP

This is the orthorhombic perovskite, $LaYO_3$ solid solution.

α-M_2O_3

This is hexagonal α-La_2O_3 and Gd_2O_3 solid solution dissolving Ca, Mg, Y and Zr.

β-M_2O_3

This is monoclinic β-Gd_2O_3 dissolving Al, Ca, Co, La, Mg, Y and Zr.

c-M_2O_3

This is Mn_2O_3, cubic Gd_2O_3 and Y_2O_3 solid solution dissolving Al, Ca, Co, Cr, Fe, La, Mg, Ni, Y and Zr.

h-M_2O_3

This is hexagonal La_2O_3, Gd_2O_3 and Y_2O_3 solid solution dissolving Ca, Mg, Mn and Zr.

x-M_2O_3

This is x-La_2O_3 and high-temperature cubic Gd_2O_3 solid solution dissolving Ca, Mg, Y and Zr.

Melilite

This is Gehlenite ($Ca_2Al_2SiO_7$), Fe-Gehlenite ($Ca_2Fe_2SiO_7$), Åkermanite (Ca_2MgSiO_7), Fe-Åkermanite (Ca_2FeSiO_7) and $Ca_2CoSi_2O_7$.

MgF_2

This is $(Co,Fe,Mg,Mn,Ni,V)F_2$.

$Mg_2P_2O_7$ (α and β)

This is α and β-$Mg_2P_2O_7$ dissolving Ca.

$Mg_2V_2O_7$

This is $(Co,Mg,Ni)_2V_2O_7$.

$Mg_3P_2O_8$

This is $Mg_3P_2O_8$ dissolving Ca.

$Mg_3V_2O_8$

This is $(Co,Mg,Ni)_3V_2O_8$.

$MgWO_4$-type

This is (Al,Fe)NbO_4 and (Co,Fe,Mg,Mn,Ni)WO_4 solid solution. Prototype $MgWO_4$.

$Mn_4Nb_2O_9$

This is $(Co,Fe,Mg,Mn)_4Nb_2O_9$.

MoS_2

This is $(Mo,W)S_2$ solid solution.

Mullite

Mullite (around $Al_6Si_2O_{13}$) solid solution dissolving Fe.

Nb_2O_5

This is Nb_2O_5 dissolving Mg and V.

Ni_6MnO_8-type

This is $(Mg,Ni)_6MnO_8$.

Ni_7S_6

This is Ni_7S_6 dissolving Fe.

Ni_9S_8

This is Ni_9S_8 dissolving Fe.

$NiMnO_3$

This is $NiMnO_3$ with Ilmenite structure.

$NiNb_2O_6$

This is $NiNb_2O_6$. This phase has the same structure as the Nb_2FeO_6 phase, but is modeled separately.

NiV_2O_6

This is $(Co,Ni)V_2O_6$.

Olivine

This is Calcio-olivine (Ca_2SiO_4) – Co_2SiO_4 – Fayalite (Fe_2SiO_4) – Forsterite (Mg_2SiO_4) – Tephroite (Mn_2SiO_4) – Ni_2SiO_4 – Kirschsteinite ($CaFeSiO_4$) – Monticellite ($CaMgSiO_4$) solid solution dissolving Cr and Cu.

Pentlandite

This is ternary $(Fe,Ni)_9S_8$.

Perovskite

This is $(Cr,Fe,Mn)LaO_3$.

Pyrite

This is Cattierite (CoS_2), Pyrite (FeS_2) – Hauerite (MnS_2) – Vaesite (NiS_2).

Pyrochlore

This is $(Gd,La)_2Zr_2O_7$ solid solution dissolving Y.

Pyroxenes

Modeling of low clino-pyroxene, clino-pyroxene, ortho-pyroxene and proto-pyroxene solid solutions taking into account the distribution of cations between different sublattices.

Low clino-pyroxene: This is low clino-enstatite ($MgSiO_3$) and low clino-diopside ($CaMgSi_2O_6$).

Clino-pyroxene: This is clino-enstatite ($MgSiO_3$), clino-ferrosilit ($FeSiO_3$), diopside ($CaMgSi_2O_6$), niopside ($CaNiSi_2O_6$), pigeonite ($(Mg,Fe,Ca)Si_2O_6$), hedenbergite ($CaFeSi_2O_6$) dissolving Co.

Ortho-pyroxene: This is enstatite ($MgSiO_3$) and ortho-diopside ($CaMgSi_2O_6$) with Fe solubility.

Proto-pyroxene: This is proto-enstatite ($MgSiO_3$) and proto-diopside ($CaMgSi_2O_6$) dissolving Co, Cr and Fe.

Pyrrhotite

This is Pyrrhotite (FeS) – CoS – CrS– NbS – NiS – VS solid solution dissolving Al, Cu, Gd, Mg, Mn and Zr.

Quartz

This is SiO_2 with solubility of $AlPO_4$.

Rhodonite

This is $MnO.SiO_2$ dissolving Ca, Co, Fe and Mg.

Rutile

This is MnO_2 – NbO_2 – high temperature VO_2 solid solution dissolving Fe.

Spinel

This is the cubic AB_2O_4-type spinel solid solution containing Al-Ca-Co-Cr-Cu-Fe-Mg-Mn-Ni-O. Distribution of cations between tetrahedral and octahedral sites, as well as vacancies on the octahedral sites to model deviation from the ideal stoichiometry toward higher oxygen potential and interstitial Fe to model deviation toward excess iron are taken into account.

This is Spinel ($MgAl_2O_4$), Magnetite (Fe_3O_4), Cuprospinel ($CrFe_2O_4$), Hercynite ($FeAl_2O_4$) and many more.

Thio-spinel

This is the sulfur spinel. This has the same structure as the oxygen-spinel, but is modeled as a separate phase. This is $(Cu,Fe,Mn)Cr_2S_4$ – Co_3S_4 – $FeNi_2S_4$ – Ni_3S_4.

Tridymite

This is SiO_2 with solubility of $AlPO_4$.

V_3O_5-HT

This is high temperature V_3O_5 dissolving Al, Cr and Mn.

V_4O_7

This is V_4O_7 dissolving Al and Mn.

VO_2-LT

This is low temperature VO_2, MoO_2 and WO_2.

Wollastonite

This is $CaSiO_3$ dissolving Fe, Mg and Mn.

YAG

This is $(Gd,Y)_3(Al,Fe)_5O_{12}$ solid solution dissolving Cr and La.

YAM

This is $(Gd,Y)_4Al_2O_9$ and Cuspidine ($Ca_2Y_2Si_2O_9$) solid solution dissolving La.

YAP

This is (Gd,Y)(Al,Co,Cr,Fe)O_3 solid solution dissolving Ca, Mn and La.

Y_3NbO_7

This is Y_3NbO_7 solid solution with excess Nb_2O_5 and Y_2O_3.

$YNbO_4$

This is $YNbO_4$ solid solution with excess Y_2O_3.

Zircon

This is Zircon ($ZrSiO_4$) and (Gd,Y)PO_4 solid solution.

m-ZrO_2

This is monoclinic ZrO_2 solid solution dissolving Al, Ca, Cr, Gd, La and Y.

t-ZrO_2

This is tetragonal ZrO_2 solid solution dissolving Al, Ca, Cr, Fe, Gd, La, Mg, Mn, Ni and Y.

Stoichiometric Compounds

203 stoichiometric compounds are modeled in the database.

AF	CAV4O9	FE4P6O21	NINB68O171
AL2S3	CAVO3	FE3PO7	NIOCALITE_C10NS6
AL2SIO4F	CAWO4	FEP3O9	NI3P2O8
ALF3_S2	CA3WO6	FE2P2O7	NI2P2O7
ALNB11O29	CA2ZRSI4O12	FEP2O6	NIS_LT
ALNB49O124	CA3ZRSI2O9	FE3P2O8	P2O5_H
ANDALUSITE	CA6ZR19O44	FE18P2O24	P2O5_O
ANILITE	CAZR4O9	FE7P6O24	P2O5_OP
ANORTHITE	CO1LA2O4	FE2PO5	P2S5
AL3PO7	CO3LA4O10	FE7P8O28	PSEUDO_WOLLASTONITE
ALP3O9	CF2	FE3P4O14	Q_ALMGZRO
AL2P6SI4O26	CHALCOCITE_ALPHA	FEV2O6	RANKINITE
C11A7F	CHALCOCITE_BETA	GUGGENITE	SAPPHIRINE
C13A6Z2	CO3P2O8	KYANITE	SILLIMANITE
C1A8M2	CO2P2O7	LAAL11O18	SI3P4O16
C2A14M2	COVELLITE	LA1S2	SIP2O7_MONO
C3A2M1	CRNB25O64	LA2CR3O12	SIP2O7_TETR

C3A3F	CRNB49O124	LA2CRO6	SIP2O7_CUB
C4WF4	CRNB9O24	LA2NB12O33	SIS2
C4WF8	CR3P2O8	LA3NBO7	V2O_SS
CA2ALNBO6	CRP3O9	LA4SI3O12	V2O5
CA3COAL4O10	CR4P6O21	LAFE12O19	V3O5_LT
CACRSI4O10	CRPO4	LANB3O9	V3O7
CACU2O3	CR3PO7	LANBO4	V52O64
CA15CU18O35	CR5PO10	LANIO3	V5O9
CA2CUO3	CR1S1	LARNITE	V6O11
CA4MG2P6O21	CR5S6	MERWINITE	V6O13
CAMG3O16S4	CR7S8	MG2NB34O87	V7O13
CAMN2O4	CRVO4	MG5NB4O15	V8O15
CA2NB2O7	CU2COO3	MGP2O6	WO2_72
CA3NB2O8	CU2SO4	MGP4O11	WO2_90
CA4P2O9_A	CU2SO5	MN9SI3O14S1	WO2_96
CA4P2O9_B	CU2Y2O5	MNF2_S1	WO3_HT
CA10P6O25	CU3NB2O8	MNF3	WO3_LT
CA4P6O19	CUCRS2	MN3P2O8	Y2S2A_Y2SI2O7
CAP2O6_A	CUF	MN2P2O7	Y2S2B_Y2SI2O7

CAP2O6_B	CUFES2_LT	MNP2O6	Y2S2D_Y2SI2O7
CAP2O6_G	CUGD2O4	MN2V2O7	Y2S2G_Y2SI2O7
CA2P6O17	CUNB2O6	MNYO3_HEX	Y2SIO5
CAP4O11_A	CU3P2O8	MOF4	ZR11NB4O32
CAP4O11_B	CUPO3	MO4O11	ZR13NB4O36
CA7P2SI2O16	CU2P2O7	MO8O23	ZR15NB4O40
CA10SI3O15F2	CUPRITE	MO9O26	ZR3Y4O12
CA5SI2O8F2	CUSPIDINE	MOO3	ZR5NB2O15
CA2V2O7	CW3F	MO2S3	ZR6NB2O17
CA3V2O8	CWF	NBF5	ZR7NB2O19
CA4V2O9	DJURLEITE	NBO	ZR8NB2O21
CA10V6O19	FEAL2S4	NI3S2_LT	ZRF4
CA9V6O18	FENB25O64	NI4NB2O9	ZRO8S2
CAV2O5	FENB49O124	NINB14O36	ZRS2
CAV3O7	FENB9O24	NINB36O91	